



ELSEVIER

1 February 1997

OPTICS  
COMMUNICATIONS

Optics Communications 135 (1997) 121–127

# Reconstruction of the transverse dynamics of a bimode CO<sub>2</sub> laser

C. Lepers<sup>a,1</sup>, V. Zehnlé<sup>a</sup>, D. Hennequin<sup>a</sup>, D. Dangoisse<sup>a</sup>, A. Barsella<sup>b</sup>,  
E. Arimondo<sup>b,2</sup>

<sup>a</sup> *Laboratoire de Spectroscopie Hertzienne, Centre d'Etudes et de Recherches Lasers et Applications,  
Université des Sciences et Technologies de Lille, F-59655 Villeneuve d'Ascq Cedex, France*

<sup>b</sup> *Dipartimento di Fisica, Università di Pisa, I-56126 Pisa, Italy*

Received 3 July 1996; accepted 3 September 1996

## Abstract

Temporal evolution of the laser electric field at any point of the transverse plane of a bimode CO<sub>2</sub> laser is reconstructed using three fast detectors located at different points in the transverse plane. We investigated a situation in which the dynamics is particularly rich i.e. displaying different periodic and chaotic regimes. A comparison between numerical analysis and experiments allows us to perform a critical evaluation of the method.

## 1. Introduction

In the past few years, the spatio-temporal nonlinear dynamics of lasers have been intensively studied [1–5]. In particular, the transverse dynamics, where the laser electric field varies at different points of the transverse plane, contains important nonlinear features, strongly linked to the turbulence. However the experimental study of the transverse dynamics is often quite difficult due to the lack of fast-response-detector arrays allowing the dynamics to be followed on time intervals comparable with the temporal evolution of the phenomena. For example with CO<sub>2</sub> lasers, detectors based on thermal plates are completely inadequate since they deliver only a time average intensity with time scale of 1 s for the transverse pattern whose time scale is of 1 μs. In this work we evaluate a new method using several point-like fast detectors locally set in the transverse pattern of the laser. Their outputs allow us to reconstruct the total and real-time transverse spatio-temporal dynamics.

Here, we focus on the case of a bimode laser, but the method can be extended to a multimode laser using an

adequate number of detectors. In the case of the  $q = 1$  family, corresponding to the TEM<sub>01</sub> and TEM<sub>10</sub> modes here considered, the degeneracy between the empty cavity eigenfrequencies is lifted by the cavity astigmatism. Depending on the amount of this degeneracy lift  $\Delta\nu$ , the occurrence of frequency locking leads to the so-called TEM<sub>01</sub><sup>\*</sup> hybrid doughnut mode [6–9]. This mode results from the linear bistable superposition of the TEM<sub>01</sub> and TEM<sub>10</sub> Gauss-Hermite modes with a constant optical phase difference of either  $+\pi/2$  or  $-\pi/2$  [10,11]. On the other hand, far from degeneracy i.e. for high  $\Delta\nu$  values, the intensity of the electric field oscillates periodically at the beat frequency  $\Delta\nu_b \approx \Delta\nu$  between the modes. In that case, a so-called “unlocked” doughnut is created whose dynamical temporal behavior is given by three characteristic variables corresponding to the modal amplitudes of each mode and the optical phase difference  $\Phi$  between the modes.

In the experiments of Ref. [12], two fast detectors have been used to investigate the phase or antiphase dynamics of a bimode laser. But this method does not permit to derive the time evolution of  $\Phi$  since at least three simultaneous measurements are needed to follow three variables. Here, we monitor the spatio-temporal dynamics of a bimode laser with three fast detectors, two on the nodal lines of the pattern and one on the first bisectrix. From the detected signals, the time evolution of three relevant vari-

<sup>1</sup> E-mail: lepers@lsh.univ-lille1.fr.

<sup>2</sup> E-mail: arimondo@ipifidpt.unipi.difi.it.

ables allows us to reconstruct the time evolution of the electric field at any point of the transverse plane. In analogy with Tamm's study [11], we have chosen a class B laser, in our case a CO<sub>2</sub> laser. When some specific experimental conditions for the relaxation rates are met, Tamm has shown that a bimode HeNe laser produces a period-doubling cascade leading to chaos while decreasing  $\Delta\nu$ . In the CO<sub>2</sub> laser with saturable absorber (LSA) which is considered here, similar experimental conditions have been reached. It has been noticed that the LSA also follows a period-doubling cascade as a function of  $\Delta\nu$  just before reaching the locking condition.

Our reconstruction method has been tested on numerically generated data. Thus in the first part of this work, the theoretical description of the laser is given in the framework of the so-called modal expansion [13], and numerical results are reported and analysed. Moreover, the sensitivity of misalignment or misposition of the detectors has been investigated. In the second part, we report the experimental spatio-temporal behavior of the "unlocked" doughnut, far and near locking, and we analyze the temporal evolution of the three characteristic variables mentioned above in order to illustrate the interest of the technique.

## 2. Numerical analysis

We consider a bimode class B laser which is governed by the mutual interaction of the transverse TEM<sub>01</sub> and TEM<sub>10</sub> Gauss-Hermite modes noted to as  $B_1(\rho, \varphi)$  and  $B_2(\rho, \varphi)$ :

$$\begin{aligned} B_1(\rho, \varphi) &= \left(\frac{2}{\pi}\right)^{1/2} 2\rho \exp(-\rho^2) \cos \varphi, \\ B_2(\rho, \varphi) &= \left(\frac{2}{\pi}\right)^{1/2} 2\rho \exp(-\rho^2) \sin \varphi, \end{aligned} \quad (1)$$

where  $\rho$  and  $\varphi$  are the polar coordinates in the transverse plane, i.e. perpendicular to the  $z$  axis of the cavity, and the radial coordinate  $\rho$  is normalized with respect to the beam waist. The laser field  $E$  may be written as

$$E(\rho, \varphi, z, t) = F(\rho, \varphi, t) \exp[i(k_0 z - \omega_0 t)] + \text{c.c.}, \quad (2)$$

where  $F$  is the slowly varying envelope of the field, independent of  $z$  in the mean field limit. The reference frequency  $\omega_0$  is the degenerate eigenfrequency of the modes TEM<sub>10</sub> and TEM<sub>01</sub> in absence of astigmatism and  $k_0$  is the related wave-vector. The following modal expansion is considered, as analysed in detail in Ref. [13]:

$$F(\rho, \varphi, t) = g_1(t)B_1(\rho, \varphi) + g_2(t)B_2(\rho, \varphi), \quad (3)$$

where  $g_1(t)$  and  $g_2(t)$  are the complex modal amplitudes of modes  $B_1$  and  $B_2$  respectively. From Refs. [13] and

[16], the temporal evolution of these amplitudes is governed by

$$\frac{dg_i}{dt} = -\kappa \left[ (1 + a_i)g_i - \int d\varphi \int \rho d\rho B_i(\rho, \varphi) (AP - \bar{A}\bar{P}) \right], \quad (4)$$

with  $i = 1, 2$  and where  $\kappa$  is the field relaxation rate,  $A$  the pump parameter and  $P$  the polarisation of the active medium.  $\bar{A}$  and  $\bar{P}(\rho, \varphi, t)$  are the absorption coefficient and polarisation of the saturable absorber respectively. In order to take care of the astigmatism present in the experiments, we introduced the detunings  $a_i$  given by

$$a_i = \frac{\omega_i - \omega_0}{\kappa}, \quad (5)$$

where  $\omega_1$  and  $\omega_2$  stands for the empty cavity frequency of modes  $B_1$  and  $B_2$  respectively. Eq. (4) is coupled to the Bloch equations for the active medium and saturable absorber. The active medium of a class B laser is modeled by an equation for the population inversion where the adiabatic elimination of  $P$ ,  $P = FD$ , has been performed:

$$\frac{dD}{dt} = -\gamma_{\parallel} (|F|^2 D + D - 1). \quad (6)$$

For the absorbing medium, we consider the simplest description with both polarisation  $\bar{P}$  and population inversion  $\bar{D}$  adiabatically eliminated, leading to

$$\bar{P} = \frac{F}{1 + a|F|^2}, \quad (7)$$

where  $a$  is the relative saturability of the absorber with respect to the active medium. The set of integro-differential equations given by Eqs. (4)–(7) has been solved numerically and the dynamical regimes of the laser are analysed with respect to the frequency difference  $\Delta\nu$  between the modes:

$$\frac{\Delta\nu}{\kappa} = \frac{a_2 - a_1}{2\pi}. \quad (8)$$

Writing the complex modal amplitudes as  $g_i = \sqrt{I_i} \exp(i\varphi_i)$  ( $i = 1, 2$ ), the relevant variables considered throughout this paper are the modal intensities  $I_i$ , and the relative phase between the modes  $\Phi = \varphi_1 - \varphi_2$ . In order to display synthetically the dynamical regimes of the laser as well as to locate the control parameter range where the transverse pattern of the LSA exhibits instabilities, a theoretical bifurcation diagram is shown in Fig. 1a. The maxima of the temporal signal  $I_1(t)$  are reported versus the control parameter  $\Delta\nu$  which has been swept for increasing and decreasing values. Other LSA parameters have been chosen to match with the experimental situation. When  $\Delta\nu$  is high ( $\Delta\nu > 29.8 \times 10^{-3}\kappa$ ), the dynamical regime is periodic. As  $\Delta\nu$  decreases ( $29.8 \times 10^{-3} < \Delta\nu/\kappa < 23.7 \times 10^{-3}$ ), a period doubling bifurcation followed by chaos occurs. At lower  $\Delta\nu$  values, the system jumps on different

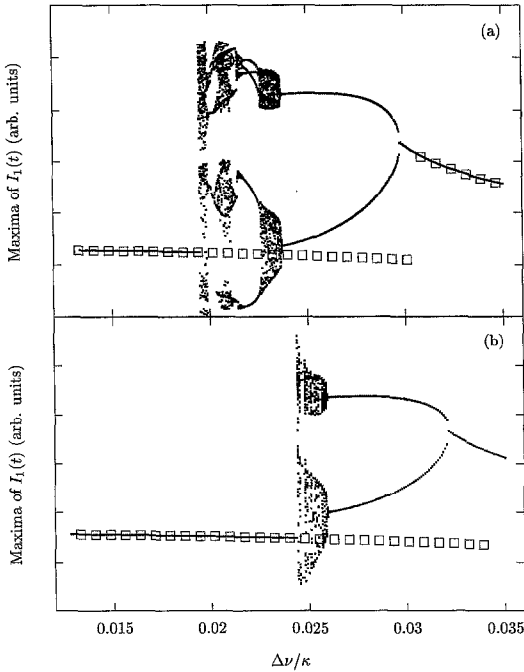


Fig. 1. Bifurcation diagram showing the temporal maxima of  $I_1(t)$  as a function of the control parameter  $\Delta\nu$  swept increasingly (squares) and decreasingly (dots) for (a) the LSA and (b) the laser without saturable absorber. The numerical integration has been performed with the following set of laser parameters: in (a)  $A = 2$ ,  $\bar{A} = 0.5$ ,  $a = 20$  and  $\gamma_{||} / \kappa = 0.1$ ; in (b) same parameters except  $\bar{A} = 0$ .

periodic and chaotic attractors. Finally at  $\Delta\nu$  smaller than  $19.5 \times 10^{-3}\kappa$ , frequency locking occurs, resulting in a stationary behavior. When  $\Delta\nu = 0$ , both stationary phase values  $\Phi = \pm \pi/2$  are simultaneously stable and the laser output patterns are doughnuts of right and left helicities. When  $\Delta\nu$  is increased starting from zero, the bifurcation sequence corresponds first to a stationary solution, stable up to  $\Delta\nu = 30.3 \times 10^{-3}\kappa$ , and for higher  $\Delta\nu$  to a periodic solution. As shown in Fig. 1a, bistability is found between the stationary branch and the periodic or chaotic attractors for  $19.5 \times 10^{-3} < \Delta\nu/\kappa < 30.3 \times 10^{-3}$ , a feature which has also been evidenced in the experiments.

Let us illustrate the effect of the saturable absorber on the laser dynamics. Fig. 1b is the bifurcation diagram of a laser without absorber i.e. all parameters are the same as in Fig. 1a except  $\bar{A} = 0$ . While decreasing  $\Delta\nu$ , we observe periodic solutions, then a narrow chaotic window and finally a stationary branch. The comparison with Fig. 1a shows clearly that the different temporal behaviors are closely related to the presence of a saturable absorber inside the cavity.

The intensity of the electric field at the point  $P(\rho, \varphi)$  on the transverse pattern reads

$$I_{\rho, \varphi}(t) = |F|^2 = G(\rho) \left[ I_1 \cos^2 \varphi + I_2 \sin^2 \varphi + \sqrt{I_1 I_2} \cos \Phi \sin 2\varphi \right], \quad (9)$$

where

$$G(\rho) = \frac{8}{\pi} \rho^2 \exp(-2\rho^2). \quad (10)$$

The first two terms of  $I_{\rho, \varphi}$  are proportional to the intensities of the two modes respectively, and the last one is an interference term. The relevant variables  $I_1$ ,  $I_2$  and  $\Phi$  may be obtained from the intensity measurements  $I_{\rho, 0}$ ,  $I_{\rho, \pi/4}$  and  $I_{\rho, \pi/2}$  given by the three detectors. Indeed, from (10) we get

$$I_1 = \frac{I_{\rho, 0}}{G(\rho)}, \quad I_2 = \frac{I_{\rho, \pi/2}}{G(\rho)}. \quad (11)$$

The phase  $\Phi$  may be obtained from the  $I_{\rho, \pi/4}$  intensity:

$$\cos \Phi = \frac{2I_{\rho, \pi/4} - I_{\rho, 0} - I_{\rho, \pi/2}}{2\sqrt{I_{\rho, 0} I_{\rho, \pi/2}}}. \quad (12)$$

Note that Eq. (12) does not give the sign of  $\Phi$ , but as it does not appear in Eq. (9), this is not a problem. The key idea of the experiments is to reconstruct the pattern in the whole transverse plane by putting these results back into (10). Note that other configurations of the three detectors may be also used at the price of a less direct connection between the relevant variables and the detectors outputs.

Practically, difficulties may arise if the position of the detectors is not perfectly known. The importance of this effect has been determined through a numerical study. In order to simulate experimental conditions, let us suppose that the intensities  $I_{\rho, 0}$ ,  $I_{\rho, \pi/4}$  and  $I_{\rho, \pi/2}$  are given by detectors located at three positions corresponding to a slight angular displacement from the nodal lines and their bisectrix. Using these numerical data, we derive from Eq. (11) and Eq. (12) a new set of relevant variables  $I'_1$ ,  $I'_2$  and  $\Phi'$ , to be compared with  $I_1$ ,  $I_2$  and  $\Phi$ . As an illustration, Fig. 2 displays the temporal  $T$  periodic signals  $I_1$  and  $|\Phi|$  and their counterparts  $I'_1$  and  $|\Phi'|$  reconstructed from the signals taken at  $\varphi = 8^\circ$ ,  $82^\circ$ ,  $45^\circ$  and  $\varphi = 18^\circ$ ,  $87^\circ$ ,  $45^\circ$  respectively. These angular displacements have been chosen far above the accuracy with which the detectors can be located. This test demonstrates that the method allows a faithful reconstruction of amplitude and phase evolutions even if the detectors are slightly mispositioned, the only effect being a slight distortion of the signals, not sufficient to hide the underlying dynamics. From these data, we have also obtained using Eq. (9) the transverse pattern and checked the good comparison between both cases.

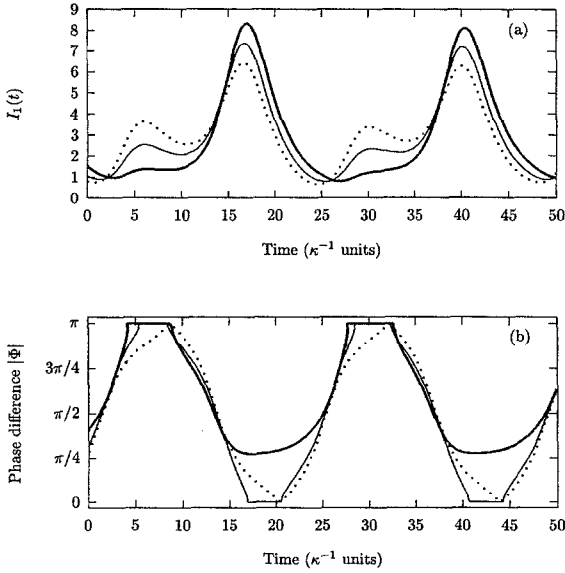


Fig. 2. Temporal evolution of (a) the modal intensity  $I_1(t)$  and (b) absolute phase  $|\Phi(t)|$  for  $\Delta\nu = 0.025$ . Laser parameters are the same as in Fig. 1 except  $\bar{A} = 0.6$ . Normal, dotted and bold lines correspond to data evaluated at azimuthal angles  $\varphi = (0^\circ, 90^\circ, 45^\circ)$ ,  $(8^\circ, 82^\circ, 45^\circ)$  and  $(18^\circ, 87^\circ, 45^\circ)$  respectively. In (b), the plateaus arise at  $\Phi' = 0$  and  $\pi$  because the function  $\cos[\Phi'(t)]$  derived from Eq. (12), if greater (lower) than 1 ( $-1$ ), is set to 1 ( $-1$ ).

In conclusion, stronger distortion of the phase evolution is possible in the case that the detector signals suffer from some rescale/translation effect. In this case the main effects are to distort the phase evolution so that it does not extend to the complete  $[0, 2\pi]$  interval, but the underlying dynamics still remains clearly visible.

### 3. Experiments

The single line CO<sub>2</sub> laser is composed of a Fabry-Perot resonator limited by a plane mirror which acts as an output coupler and a grating [14]. Two lenses inserted in the cavity, one of which is mounted on a rotation/translation stage, allow the transverse mode spacing between the TEM<sub>00</sub> and TEM<sub>01</sub>\* modes to be continuously changed. Note that the aperture of the intracavity iris limits the transverse modes oscillating in the cavity to the TEM<sub>00</sub>, TEM<sub>01</sub> and TEM<sub>10</sub>. The transverse mode spacing between the  $q = 0$  and  $q = 1$  families is around 20 MHz. Although the amplifier cell is closed by antireflection coated plates in order to keep astigmatism of the cavity at a level as low as possible, a frequency degeneracy lift  $\Delta\nu$  between the modes of the family  $q = 1$  occurs. Astigmatism may be partially or totally compensated by tilting and translating the lens. Note that experimentally, we cannot measure the frequency difference  $\Delta\nu$  between empty cavity modes, but only the beat frequency  $\Delta\nu_b$  between the laser modes,

which is in most cases close to  $\Delta\nu$ , the main exception being locking. Control of astigmatism allows  $\Delta\nu_b$  to be varied continuously in the range 0.1 to 1 MHz. When there is locking,  $\Delta\nu_b = 0$ ;  $\Delta\nu_b$  never takes a value between 0 and 100 kHz, because of locking. In this laser without intracavity saturable absorber, a period-doubling regime is observed in a very narrow range of the cavity length variation around  $\Delta\nu_b = 100$  kHz, in good agreement with Fig. 1b.

Osmium Tetroxide (OsO<sub>4</sub>) has been introduced at a low pressure as an intracavity saturable absorber in order to increase the range of the parameter space in which instabilities are observed. In these conditions, the laser is tuned on the 10P14 line of the 10.6  $\mu\text{m}$  branch, to keep the laser emission in coincidence with the strongest OsO<sub>4</sub> absorption. Let us recall that in a monomode TEM<sub>00</sub> CO<sub>2</sub> LSA, three main temporal regimes are usually observed depending on the absorber pressure  $p_{\text{abs}}$ . At low pressure ( $p_{\text{abs}} < 30$  mTorr), the laser is stable and delivers a time independent output. When the pressure is increased, the system undergoes a Hopf bifurcation and a sinewave modulation is created. At higher pressure ( $p_{\text{abs}} > 100$  mTorr), the temporal regime is a self-pulsing regime called passive Q-switching (PQS) in which the time evolution of the laser intensity exhibits very different shapes depending on the operating point [15]. The present experiments on the bi-mode LSA have been performed in the lower pressure range, where the monomode TEM<sub>00</sub> LSA delivers a time independent output. In good agreement with the numerical simulations, we have observed in this case period doubling and chaos in a wider range of variation of  $\Delta\nu_b$  ( $60 < \Delta\nu_b < 120$  kHz) than in the case of the laser without absorber.

Using three HgCdTe infrared detectors, we have followed the temporal evolution of the intensities at the  $P_{\rho,0}$ ,  $P_{\rho,\pi/4}$ , and  $P_{\rho,\pi/2}$  points of the “unlocked” doughnut, in order to reconstruct the real time evolution of the pattern through the three variables  $I_1$ ,  $I_2$  and  $\Phi$ . Two situations have been studied: (i) the amount of astigmatism, i.e.  $\Delta\nu$ , is swept at a fixed cavity length and (ii)  $\Delta\nu$  is kept fixed and the cavity detuning is swept.

Far from locking ( $\Delta\nu_b > 1$  MHz) and without absorber,  $I_1$  and  $I_2$  are almost time independent, as it may be expected from Refs. [4,12]. Fig. 3a shows  $I_1$  and  $I_2$  for a smaller value of  $\Delta\nu$  ( $\Delta\nu_b = 770$  kHz), when a sinewave appears superimposed on the DC component of the intensities. Fig. 3b shows that in this case,  $\Phi$  evolves linearly with time, as if it was proportional to the beat frequency. However,  $|\Phi|$  does not span the whole interval  $[0, \pi]$ . As shown in the numerical analysis, this could originate from mispositioning of the detectors. Moreover,  $I_1$ ,  $I_2$  and  $|\Phi|$  are deduced from the quantitative comparison of intensities delivered by three different detectors. We developed a calibration method allowing us to obtain the actual intensities. However, uncertainties together with a possible high frequency cutoff of the detectors could explain the limited

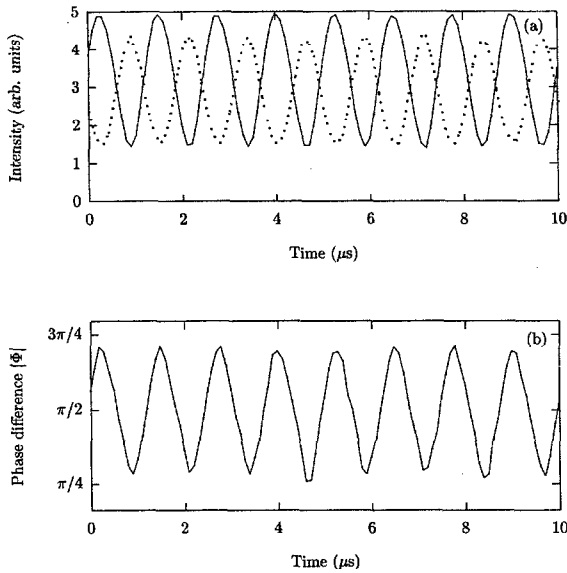


Fig. 3. Periodic oscillations far from locking ( $\Delta\nu_b = 770$  kHz): in (a), modal amplitudes of the doughnut modes of the CO<sub>2</sub> laser without absorber with the amplitude of the DC components being reduced in order to show the modal oscillations; in (b),  $|\Phi(t)|$ .

span of  $|\Phi|$  in Fig. 3b. Another possibility is that we are dealing with a behavior where the two modes do not alternate completely but coexist.

An additional problem appears in the areas where the intensities reach levels very close to 0: the signal to noise ratio decreases very much, generating very large distortion particularly on  $|\Phi|$ , as the zero intensity value is a critical point where the phase is not determined. In that case, the real evolution of the pattern can only be deduced by continuity.

Let us now describe the evolution of the dynamics of the LSA as a function of astigmatism. Starting from the regime described in the previous paragraph ( $\Delta\nu_b \approx 1$  MHz) and as astigmatism is decreased down to  $\Delta\nu_b = 100$  kHz, we observe that the modal amplitude oscillations increase regularly but remain periodic. This behaviour corresponds to an increase of the interaction strength between the two modes through the active medium. For  $\Delta\nu_b = 100$  kHz, it leads to the appearance of second harmonic components in

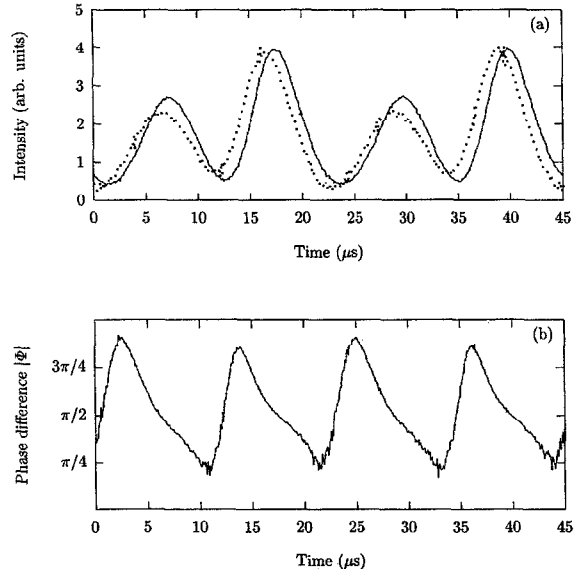


Fig. 4. Time evolution near the locked state ( $\Delta\nu_b = 100$  kHz) of the  $2T$  oscillations of the doughnut mode amplitudes, (b) of  $|\Phi(t)|$ .

the Fourier spectrum of the signal, as pointed out in Refs. [16,17]. Note that in the range 100 kHz to 1 MHz lies the relaxation frequency of the laser (about 200 kHz). Although resonance mechanisms are probably enhanced when the beat frequency is close to the relaxation frequency, it appears that the phase evolution remains linear with time. When we further decrease  $\Delta\nu_b$  the modes lock to a common frequency after a bifurcation sequence followed by chaos, as also observed numerically. Now, if starting from locking, the astigmatism is increased, the system evolves with hysteresis from a locked to an “unlocked” doughnut showing evidence of bistability between locked and unlocked states. The “route” from unlocking to locking going through a period-doubling cascade is richer than the reverse one in good agreement with the numerical simulations as shown in Fig. 1a.

Let us now consider the case where the astigmatism is kept fixed, while the cavity detuning is swept. A behaviour similar to that described above is obtained, with a period-doubling cascade observed as a function of the fine tuning

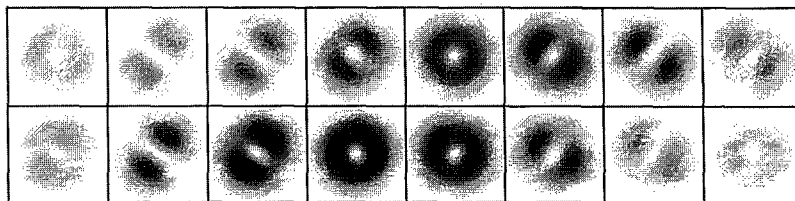


Fig. 5. Experimental pattern reconstruction over one period ( $T = 22.1$   $\mu$ s) of the unlocked doughnut in the  $2T$  regime. The time interval between successive patterns is  $1.5$   $\mu$ s.

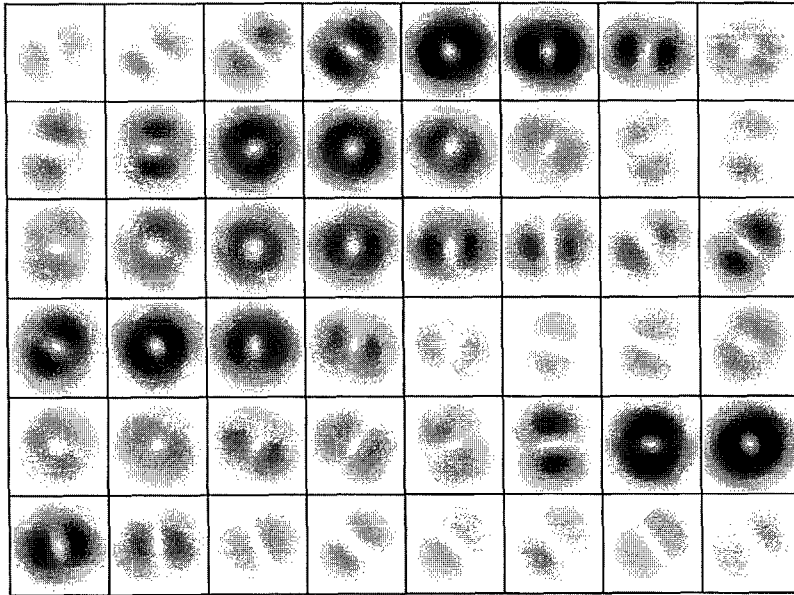


Fig. 6. Experimental pattern reconstruction over one period ( $T = 70 \mu\text{s}$ ) of the unlocked doughnut in the  $7T$  regime. The time interval between successive patterns is  $1.5 \mu\text{s}$ .

of the cavity length before the modes lock to a common frequency. The bifurcation diagram as a function of the cavity detuning shows oscillations at  $T$ ,  $2T$  and  $4T$  culminating in a chaotic behavior, inside of which a  $7T$  periodic window appears. The system emerges from chaos when the two modes lock in frequency. Fig. 4 gives an example of  $2T$  oscillations in which the signal has a phase evolution very similar to that of a rotated unlocked doughnut, with a distortion in the second part of this phase evolution making it asymmetric.

In order to analyze the spatio-temporal dynamics, we reconstruct the evolution of the transverse pattern intensity distribution in the  $2T$  periodic regime (Fig. 5). During half period of the signal, a two-spot pattern oriented along the first bisectrix is successively followed by a doughnut and a two-spot pattern oriented along the other bisectrix. This full sequence is repeated during the second half period. Rotating patterns, not shown here, are only obtained when the modal amplitudes oscillate in antiphase. As a function of the detuning of the resonator, we have observed  $7T$  periodic oscillations and the corresponding pattern evolution becomes much more complex, as shown in Fig. 6.

#### 4. Conclusion

Using three fast detectors, the spatio-temporal dynamics of a bimode laser has been examined and found in good agreement with numerical simulations. From the detected signals, we have reconstructed the time evolution

of the electric field at any point of the transverse plane. Limitations of the method arise from misalignment and calibration errors of the detectors: extending this method to family  $q = 2$  or mixed fundamental-doughnut dynamics seems now quite difficult due to the additional problems which would arise in an attempt to calibrate and align five detectors. A good qualitative agreement has been found between the theory and the experiments on the bifurcation diagrams obtained with and without intracavity absorber: saturable absorber presence expands the control parameter range in which instabilities are observed.

#### Acknowledgements

This work is part of collaboration program between the Centre National de la Recherche Scientifique (CNRS) of France and the Consiglio Nazionale delle Ricerche (CNR) of Italy. The Laboratoire de Spectroscopie Hertzienne is Unité de Recherche Associée au CNRS #249. The Centre d'Etudes et de Recherche Lasers et Applications is supported by the Ministère chargé de la Recherche, the Région Nord-Pas de Calais and the Fonds Européen de Développement Economique des Régions.

#### References

- [1] M. Brambilla, F. Battipede, L.A. Lugiato, V. Penna, F. Prati, C. Tamm and C.O. Weiss, *Phys. Rev. A* 43 (1991) 5090.
- [2] M. Brambilla, L.A. Lugiato, V. Penna, F. Prati, C. Tamm and C.O. Weiss, *Phys. Rev. A* 43 (1991) 5114.

- [3] J.R. Tredicce, E.J. Quel, A.M. Ghazawi, C. Green, M.A. Pernigo, L.M. Narducci and L.A. Lugiato, *Phys. Rev. Lett.* 62 (1989) 1274.
- [4] M. Brambilla, M. Cattaneo, L.A. Lugiato, R. Pirovano, F. Prati, A.J. Kent and G.L. Oppo, A.B. Coates, C.O. Weiss, C. Green, E.J. D'Angelo and J.R. Tredicce, *Phys. Rev. A* 49 (1994) 1427, 1452.
- [5] I. Boscolo, L.A. Lugiato, F. Prati, T. Benzoni and A. Bramati, *Optics Comm.* 115 (1995) 379.
- [6] L.A. Lugiato, G.L. Oppo, M.A. Pernigo, J.R. Tredicce and L.M. Narducci, *Optics Comm.* 68 (1988) 63.
- [7] L.A. Lugiato, C. Oldano and L.M. Narducci, *J. Opt. Soc. Am. B* 5 (1988) 879.
- [8] K. Staliunas, M.F.H. Tarroja and C.O. Weiss, *Optics Comm.* 102 (1993) 69.
- [9] G. Slekyš, K. Staliunas, M.F.H. Tarroja and C.O. Weiss, *Appl. Phys. B* 59 (1994) 11.
- [10] W.W. Rigrod, *Appl. Phys. Lett.* 2 (1963) 51.
- [11] Chr. Tamm and C.O. Weiss, *J. Opt. Soc. Am. B* 7 (1990) 1034.
- [12] D. Hennequin, C. Lepers, E. Louvergneaux, D. Dangoisse and P. Glorieux, *Optics Comm.* 93 (1992) 318.
- [13] L.A. Lugiato, G.L. Oppo, J.R. Tredicce, L.M. Narducci and M.A. Pernigo, *J. Opt. Soc. Am. B* 6 (1990) 1019.
- [14] C. Lepers, V. Zehnlé, D. Hennequin, D. Dangoisse, P. Glorieux, A. Barsella and E. Arimondo, *Nonlinear Dynamics in Lasers, Laser Optics '95*, SPIE proceedings series 2792 (1995) 215.
- [15] D. Hennequin, D. Dangoisse and P. Glorieux, *Phys. Rev. A* 42 (1990) 6966.
- [16] A. Barsella, P. Alcantara Jr, E. Arimondo, M. Brambilla and F. Prati, *Chaos, Solitons & Fractals* 4 (1994) 1665.
- [17] Chr. Tamm, *Phys. Rev. A* 38 (1988) 5960.